

## 63. *A Model Experiment on the Mechanism of Occurrence of Earthquake.*

By Seiti YAMAGUTI,

Earthquake Research Institute.

(Read June 18, 1935.—Received Sept. 20, 1935.)

### Introduction.

In a previous paper<sup>1)</sup>, we have remarked that, near the epicentres of the “deep” earthquakes, “conspicuous and rather conspicuous” earthquakes rarely occur immediately before or after the respective earthquakes, and that, three conspicuous maxima of frequencies of the latter are found in the regions at about  $-500$ ,  $500$  and  $1000$  in kilometres measured from the maximum of the former.

With regard to these results, Prof. Torahiko Terada suggested, that if a spherical part of the crust at the “deep” earthquake origin lying several hundred kilometres beneath the earth surface, happens to expand or yield by some cause, the maximum shearing stress may occur in a conical surface with semivertical angle of about  $45^\circ$  and the vertex at the centre of sphere, and the fracture may propagate along these directions towards the earth surface.

It was the first aim of the present experiment to verify these suggestions. The second object was to verify the fact already noticed by the author that, very near the thunderstorms and the cyclonic centres, and also near the region of great precipitations, earthquakes very rarely occur at the time of these meteorological occurrence, and a remarkable maximum of frequency of the latter seems to exist about several hundred kilometres apart from the formers<sup>2)</sup>.

This experiment was carried out during the period of about 15 months from March, 1934 to June, 1935.

### Method of Experiment.

Taking a rectangular wooden tank,  $T_1$ , whose sides are 20, 30 and 60 cm, and placing in it a spherical caoutchouc-balloon,  $B$ , of good

1) S. YAMAGUTI, *Bull. Earthq. Res. Inst.*, **11** (1933), 501~504.

2) *Bull. Earthq. Res. Inst.*, **12** (1934), 214~221, 742~753; **13** (1935), 569~575.

material, whose initial diameter was 4.0 cm, connected with a very fine flexible caoutchouc-tube (dia = 1.5 mm) to a open manometer, *M*, as well as to a cylindrical air chamber, *V* (dia = 4.0 cm), as shown in Fig. 1, a large quantity of agar-agar dissolved in warm water was poured into this tank and cooled for one day or two, until it solidified up to the innermost part. The bottom end of *V* is connected with a caoutchouc tube (dia = 8 mm), to a water tank, *H*, of which the head is held about 150 cm high, and the water surface in *V* is raised up gradually at the rate of 1 cm/min. The air contained in *V* and *B* is thus compressed and the balloon, *B*, was compelled to expand until

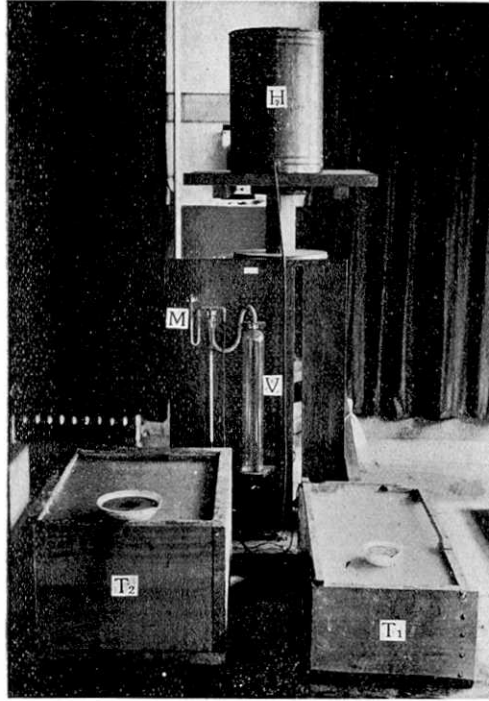


Fig. 1.

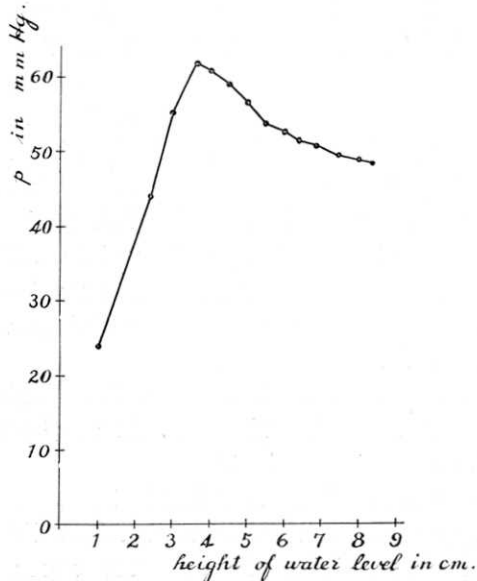


Fig. 2, a. Pressure-Water level curve.

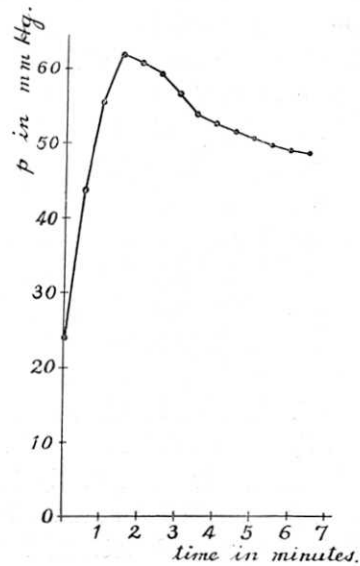


Fig. 2, b. Pressure-Time curve.

the crack was produced in agar-agar. The pressure,  $p$ , at the beginning of producing crack was read when the mercury meniscus of  $M$  begins to fall down while the water level in  $V$  is continued to rise up, which relation is shown in Fig. 2,  $a$  and  $b$ , and in Fig. 3. This photogram

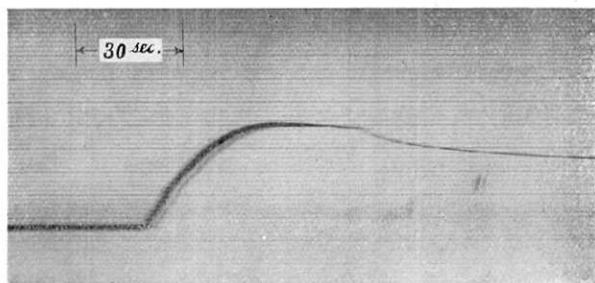


Fig. 3.

of the motion of mercury meniscus was taken by illuminating from upward, on the rolling film, which was rolled by the rate of 1 revolution per 90 seconds.

The general features of the cracks which were developed on the surface are shown in Figs. 11,  $a \sim 11, e$ . Radial gaping cracks are the tension cracks due to the bulging up of the surface, while the conical cracks shown in Figs. 11,  $a$  and 11,  $b$  are the shear cracks here interested. The configuration of the shear cracks starting from the bottom and extending to the surface were studied by cutting the agar-agar with a vertical plane through the centre of balloon, and parallel to the longest side, the angle of inclination,  $\theta$ , of the crack line from vertical, being measured.

The dry sticks of agar-agar used in one experiment, were 60 and 100 in number and 450 and 750 grams in mass for the tanks  $T_1$  and  $T_2$  respectively, the volume of  $T_2$  being  $30 \times 40 \times 50$  cubic centimetres.

To see if the crack in question really starts from the bottom but not from the surface by the tension at the surface, a glass plate with the weight of 1 kg, was put over the surface to prevent the surface cracking. It was fully recognized that the shear cracks studied grow from the inner part, very near the balloon.

From the results of about 30 experiments, the suggestion made by Prof. T. Terada, above cited, was verified, and the angle of shear crack,  $\theta$ , was found to be lying between  $40^\circ$  and  $50^\circ$ .

Next, we tried to study the variation of  $\theta$ , according to the variation of position of a surface loading which consists of a porcelain dish with hemispherical bottom, loaded with weight. In the first experiment, the depth,  $e$ , of the centre of balloon (initial diameter,  $D_0=4$

cm), from the surface was fixed at about 9 cm, and a dish,  $P$ , with radius of curvature,  $\rho=12.2$  cm, loaded with weight,  $W=2.29$  kg (weight of dish included), was put at the various distances,  $d$ , or  $r=d/e=0\cdots 3.7$ , from the so-called "epicentre" of a balloon along the centre axis of the tank,  $T_1$ . For the tank,  $T_2$ , the values of  $D_0=5$  cm,  $e=12$  cm,  $\rho=8.2$ , and  $W=2.15$  kg were taken, and the values of  $r$  was changed from zero to 2.1. Thus, the values of  $\theta$  for different  $r$ 's, were obtained and plotted against  $r$ , as shown in Fig. 4,  $a$  and  $b$  for the tanks,

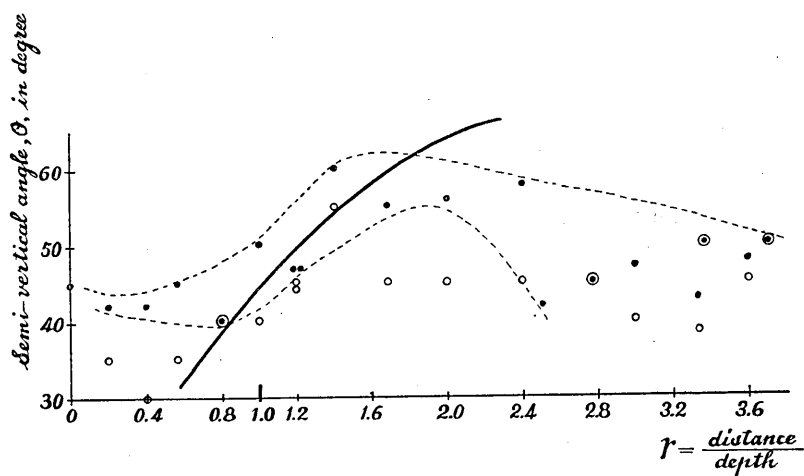


Fig. 4,  $a$ . For the first experiment with the tank,  $T_1$

$T_1$  and  $T_2$  respectively, in which the marks ● correspond to the cracks in the same side as the weight, and ○ to those in the opposite side with respect to the balloon.

In the second experiment, to make the boundary effect of the tank as small as possible, smaller values of  $D_0$ ,  $e$ ,  $\rho$  and  $W$  were taken; those were  $D_0=3.0$  cm,  $e=7$  cm,  $\rho=4.5$  cm, and  $W=1.63$  kg for the tank,  $T_1$ , and  $D_0=3.5$  cm,  $e=7$  cm,

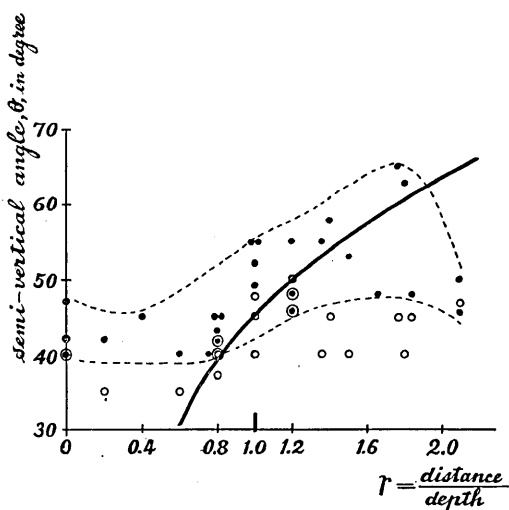


Fig. 4,  $b$ . For the first experiment with the tank,  $T_2$

$\rho=4.8$  cm, and  $W=2.07$  kg for the tank,  $T_2$ , and the similar  $\theta-r$  diagrams were drawn as shown in Fig. 5, *a* and *b*. The diameter of

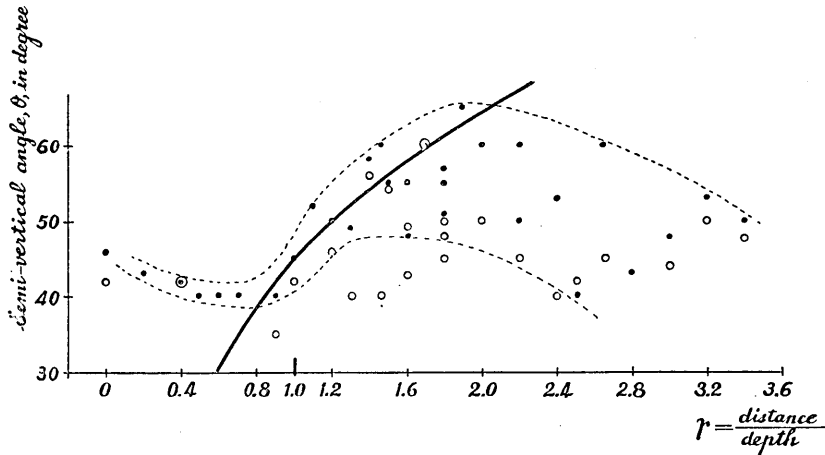


Fig. 5, *a*. For the second experiment with the tank,  $T_1$ .

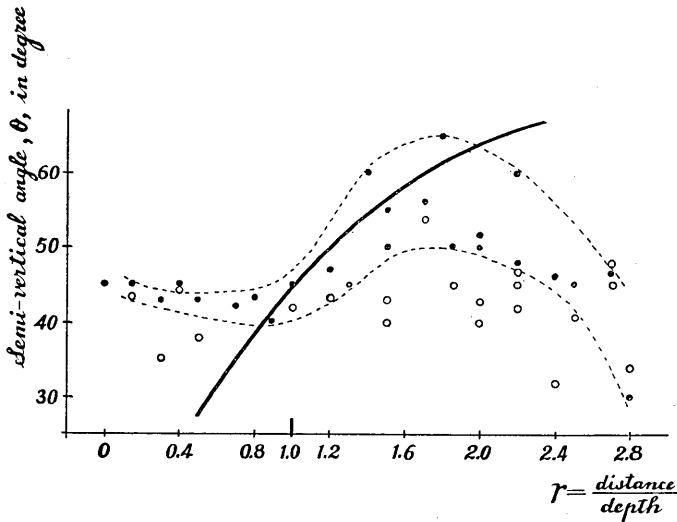


Fig. 5, *b*. For the second experiment with the tank,  $T_2$ .

the balloon at the time when the crack begins to grow, may be calculated from the equation,  $v_1 = (p_0/p_1)v_0 + (p_0/p_1 - 1) V_0 + \Delta h \cdot S$ ,

where  $v_1$  = required volume of the balloon,  
 $v_0$  = initial volume of the balloon,  
 $p_0$  = initial pressure,  
 $p_1$  = final pressure,

$S$  = sectional area of the air chamber,  
 $V_0$  = initial volume of the air chamber,  
 $\Delta h$  = change of water level,

and the final diametres of the balloon were estimated to be 4.5~5.5 in centimetres.

The frequencies of pressures, at which the cracks began to grow, falling in successive 10 mm Hg intervals, were counted and plotted as ordinates, the pressures of the intervals being taken as abscissa. These curves are shown in Fig. 6, *a*, *b* and *c* in the cases of the first

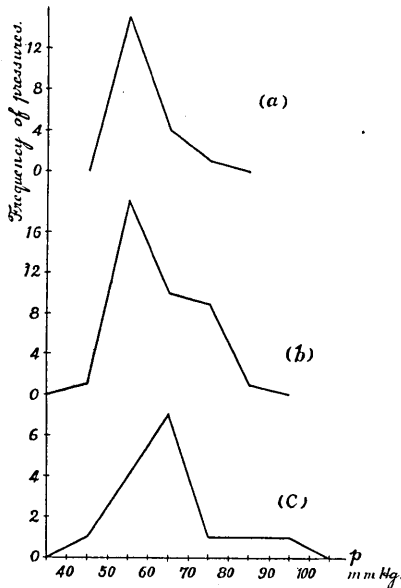


Fig. 6. With the tank,  $T_1$ .  
 (a) For the first experiment.  
 (b) For the second experiment.  
 (c) No load.

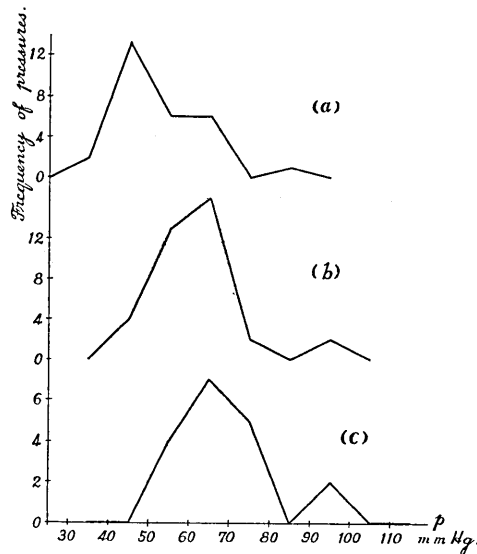


Fig. 7. With the tank,  $T_2$ .  
 (a) For the first experiment.  
 (b) For the second experiment.  
 (c) No load.

and second experiments, as well as of the experiment with no load, respectively for the tank,  $T_1$ . Similar curves are shown in Fig. 7, *a*, *b* and *c* for the tank,  $T_2$ . The curves drawn in full lines in Figs. 4 and 5, denote the values of  $\theta_0 = \text{arc tan } r$ .

Lastly, we have drawn  $p-r$  diagrams for each tank and for each experiment separately as shown in Fig. 8, *a*, *b*, and Fig. 9, *a*, *b*, in which the points marked by \* and  $\otimes$ , represent the means of  $p$  in the regions  $r > 1$  and  $r \leq 1$ , respectively. The corresponding values of  $p$  and  $r$  are shown in Table I and II.

Table I.

Table II.

For the tank, $T_1$						For the tank, $T_2$					
The first experiment			The second experiment			The first experiment			The second experiment		
$r$	$p$		$r$	$p$		$r$	$p$		$r$	$p$	
0.0	51	Mean of $p=60.0$ for $r \leq 1.0$	0.0	77	Mean of $p=64.0$ for $r \leq 1.0$	0.0	50	Mean of $p=53.2$ for $r \leq 1.0$	0.0	67.5	Mean of $p=66.2$ for $r \leq 1.0$
0.0	68		0.2	58		0.0	54		0.2	54.5	
0.2	58		0.4	58		0.0	68		0.3	61	
0.4	58		0.5	72		0.3	63		0.5	91.5	
0.6	74		0.6	59		0.4	62		0.7	57	
0.8	52		0.7	64		0.8	43		0.7	60.5	
1.0	56		0.9	54		0.8	44		0.7	61	
1.0	62		1.0	79		0.8	49		0.8	61	
							0.9		39	0.8	
1.2	52	Mean of $p=56.3$ for $r > 1.0$	1.1	51.5	Mean of $p=61.3$ for $r > 1.0$	0.8	49	Mean of $p=49.7$ for $r > 1.0$	0.9	58	Mean of $p=58.3$ for $r > 1.0$
1.2	56		1.1	57.5		1.0	50		1.0	78	
1.4	56		1.1	60.5		1.0	54		1.2	57.5	
1.7	66		1.2	66		1.0	59		1.2	62.5	
2.0	51		1.2	71		1.0	60.5		1.2	67	
2.4	56		1.2	76		1.2	40		1.3	55	
2.5	54		1.3	46		1.2	41		1.4	50.5	
3.0	50		1.3	72		1.2	46		1.5	45	
3.4	54		1.4	64		1.2	61		1.5	76	
3.4	66		1.4	59.5		1.4	44		1.7	55.5	
3.6	56		1.5	63		1.4	68		1.7	64	
3.6	58		1.5	66		1.4	48		1.8	50.5	
			1.6	65		1.7	61		2.0	48	
			1.6	67		1.8	42.5		2.0	61.5	
			1.8	51		1.8	48.5		2.0	67	
			1.8	52.5		1.8	50		2.2	50.5	
			1.8	66		2.0	58		2.2	61.5	
			1.8	75		2.1	40		2.2	62	
			1.9	54.5		2.1	48.5		2.4	47	
			2.0	72					2.5	53.5	
		2.0	76			2.5	58.5				
		2.2	58			2.7	47.5				
		2.2	72			2.7	66				
		2.4	58			2.7	68.5				
		2.5	53			2.8	64				
		2.7	59			2.8	67				
		2.8	52								
		3.0	54								
		3.2	52								
		3.4	61								

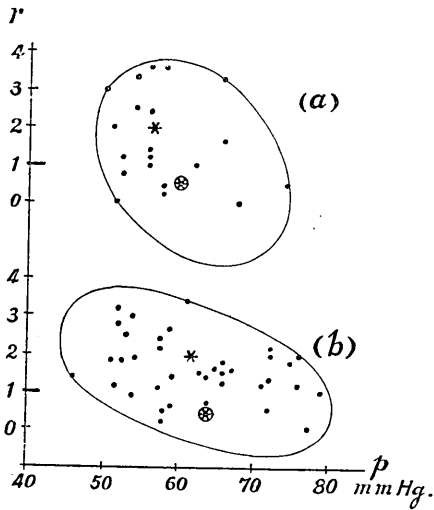


Fig. 8. With the tank,  $T_1$ .  
 (a) For the first experiment.  
 (b) For the second experiment.  
 \* : Mean for  $r > 1$   
 ⊗ : Mean for  $r \leq 1$

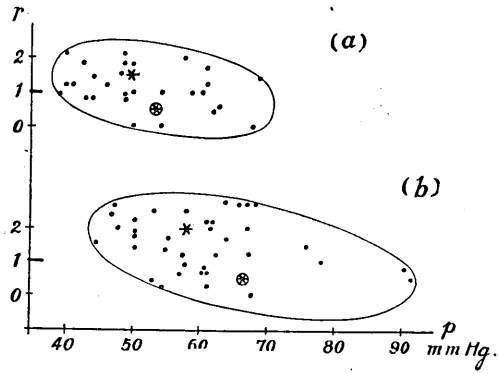


Fig. 9. With the tank,  $T_2$ .  
 (a) For the first experiment.  
 (b) For the second experiment.  
 \* : Mean for  $r > 1$   
 ⊗ : Mean for  $r \leq 1$

The forms of surface cracks are summarised and classified into 15 kinds approximately as shown in Fig. 10,  $a, b, c, \dots, n$  and  $o$ . The percentages of the occurrences of the different cracks are shown in Table III. The greatest percentage value is shown in the case of  $d$ , of which the most cracks are inclined by the angles of about  $30^\circ$  and  $150^\circ$ , and some others by the angles of about  $60^\circ$  and  $120^\circ$ , referred to the longitudinal axis of the tank.

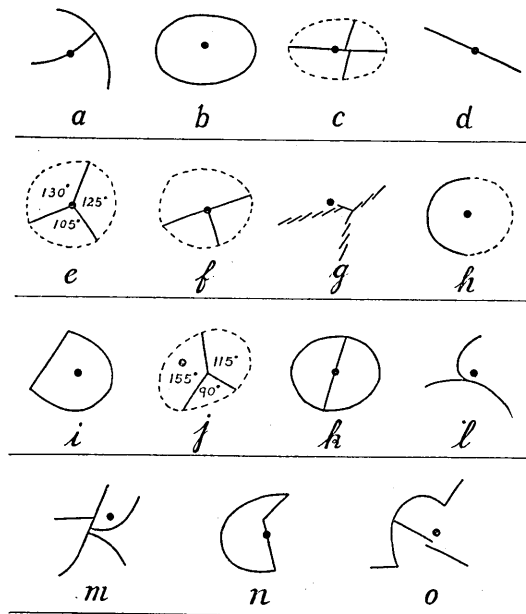


Fig. 10. Surface cracks.

Table III.

Kinds of cracks	<i>a</i>	<i>b</i>	<i>c</i>	<i>d</i>	<i>e</i>	<i>f</i>	<i>g</i>	<i>h</i>	<i>i</i>	<i>j</i>	<i>k</i>	<i>l</i>	<i>m</i>	<i>n</i>	<i>o</i>
Percentages of the occurrences	3	2	3	26	11	9	7	11	2	4	2	7	5	3	5

### Results and Discussions.

We have tried to keep the constancy of elasticity and density of agar-agar as good as possible, by taking the same initial concentration, but we found some sensible fluctuation of density in the range from 1.01 to 1.015, owing to the repeated boiling and cooling and also to the seasonal variation of room temperature. The density of agar-agar was determined by immersing, a small piece of agar-agar in the salt solution of equal density, which was measured by Baumé's pycnometer.

From Figs. 4 and 5, we may be able to say the followings:—

*a)* The values of the angles,  $\theta$ , i. e. the inclination of shear crack against the vertical are always greater in the same side as the surface load than in the opposite side with respect to the epicentre of the balloon.

*b)* The values of  $\theta$  are about  $45^\circ$  when the load is near the epicentre, that is near  $r=0$ , and they are less than  $45^\circ$ , when the load lies in the interval  $0 < r < 1$ .

*c)* The values of  $\theta$  have the tendency to approach the curve  $\theta_0 = \tan^{-1} r$ .

*d)* The values of  $\theta$  increase with  $r$ , when  $r > 1$ , until reaching a maximum value about at  $r=1.8$ , and then decrease for greater  $r$ .

*e)* Sometimes, more than one conical cracks appear at the same time, some of which have greater angles than  $\theta_0 = \tan^{-1} r$ , and others less than  $\theta_0$  (curves here omitted).

From Figs. 6 and 7, we could say that the inner pressure at the beginning of growing crack, is smaller when the surface loading is present than when it is absent, owing evidently to the effect of the initial strain due to the load.

From Figs. 8 and 9, we can see the tendency that the maximum inner pressure is less in its amount when  $r > 1$ , than when  $r \leq 1$ , which is also shown in Table I and II. This result may, for some extent, explain the fact that the occurrence of a thunderstorm, cyclone or precipitation near the epicentre is less effective in causing earthquake than the same thing occurring several hundred kilometres distant from the epicentre.

In conclusion, I wish to express my best thanks to Prof. Torahiko Terada under whose supervision the entire work has been carried out and who has given me many useful suggestions throughout the course of my investigation. I also wish to express my cordial thanks to Messrs. R. Yamamoto and T. Watanabe in the Institute of Physical and Chemical Research and also to M. Ogawa and T. Maruyama in the Imperial Higher Naval College in Tôkyô, for their kind and able assistances during the course of experiments.

### 63. 地震發生機巧に關する一つの模型實驗

地震研究所 山口 生 知

前論文に於いて著者は次の事を指摘して置いた。即ち深層地震の震源近くに於いては、其の直ぐ前後に於いて、顯著及稍顯著地震の起る事が極めて稀にして深層地震帯より測つて約  $\pm 500$  km 及 1000 km の地點に、顯著及稍顯著地震の最も起り易い處があることである。

此の結果に關して寺田寅彦博士は次の如き暗示を與へられた。若しも地下數百 km の深層地震の震源に相當する處に在る地殼の或る球形の部分が何等かの原因に依つて、膨脹或は收縮するならば、此の球の中心に頂點を持ち半頂角  $45^\circ$  なる圓錐面上に於いて最大應力が起り、地殼の破壊は之等の方向に添うて地表に向つて傳はるものと考へられる。と云ふのである。

今回の實驗の第一の目的は、此の暗示を證明せんことである。

第二の目的は、著者が既に注意して置いたことの次の事實を證明する爲めである。即ち雷雨や低氣壓の近く又は雨雪量の多い地點の近くに於いては、それ等のものゝ發生と同時に地震の起ることが極めて稀であつて、それ等の地點より數百軒隔つた處に地震が発生し易い、と云ふことを證明する爲めである。

實驗の裝置は第 1 圖に示す通り寒天を入れる角槽は容積が  $20 \times 30 \times 60$  cm<sup>3</sup> なる木製の角槽を用ひ、其の中に良質の丸いゴム球を入れ、熱湯に溶した寒天を注ぎ込みたる後 1 日或は 2 日間放置して自然に凝固させる様にした。

而してゴム球の一端は細いゴム管で壓力計に連絡し、同時に圓筒形の空氣室の上端に繋がる様にした。而して空氣室の下端は直徑 8 mm のゴム管を用ひて高所にある水槽 H に連絡し空氣室の下端の水面を徐々に上昇せしめて、角槽の中のゴム球を膨脹させることが出来る様にしたものである。かくして寒天の内部に於いて割目の發生する時の壓力は、氣筒下部の水面が上り續けて居るにも拘はらず、壓力計内の水銀頭が下り始める時を以つて其の壓力の讀とした。

剪斷力に依る割目の形は風船の中心を通り角槽の長さの方向に平行な鉛直面で、切つて見ると球心を通る鉛直線と約  $45^\circ$  の角度をなし、底から出發して表面まで届いて居ることが確かめられた。即ち約 30 回の實驗の結果に依り先に述べた寺田博士の暗示を證明することが出來た。而して此の角度  $\theta$  の大きさは  $40^\circ$  から  $50^\circ$  の間にあることが分つた。

次に寒天の表面に半球形の底を有する陶器製の皿を置き其中に錘を乗せたものを角槽の中心線上色々の場所に動かして見た時の、角度 $\theta$ の變化を研究した。

又ゴム風船の眞上より皿の中心までの距離と寒天の表面よりゴム風船の中心までの深さとの比をさり此の比の値 $r$ と、割目の發生する時の壓力 $p$ との關係を調べて見た。

之等の結果は次の通りである

1) 剪斷力に依る割目の線が鉛直線と傾く角度 $\theta$ の値は風船の中心に對して表面荷重と同じ側は反對側よりもいつでも大きい。

2) 荷重が風船の眞上にある時は $\theta$ の値は約 $45^\circ$ にして、 $0 < r < 1$ の間に於いては $45^\circ$ より小である。

3)  $\theta$ の値は $\theta_0 = \tan^{-1}r$ なる曲線に近づく傾向を持つて居る。

4)  $r > 1$ なる時は、 $\theta$ の値は $r$ と共に増加し $r=1.8$ 邊で一つの最大値をさりそれより次第に減ずる。

5) 時には圓錐形の割目が二つ以上出来るこゝがあり一つは $\theta_0 = \tan^{-1}r$ より大に他は $\theta_0$ より小なるこゝが多い。

6) 割目が發生する時の壓力 $p$ の値は、表面荷重が有る時は無い時よりも小である之は明らかに荷重に依る最初の歪の影響であるを考へられる。

7) 最大内壓 $p$ の値は表面荷重の位置に依つて異なり $r > 1$ なる時は $r \leq 1$ なる時よりも小なる様な傾向がある。

此の結果は雷や、低氣壓或は雨雪量等が震源近くに起つた時よりも、數百軒距つた遠方に發生した時の方が地震が起り易いと云ふ事實を幾分説明するものと思はれる。

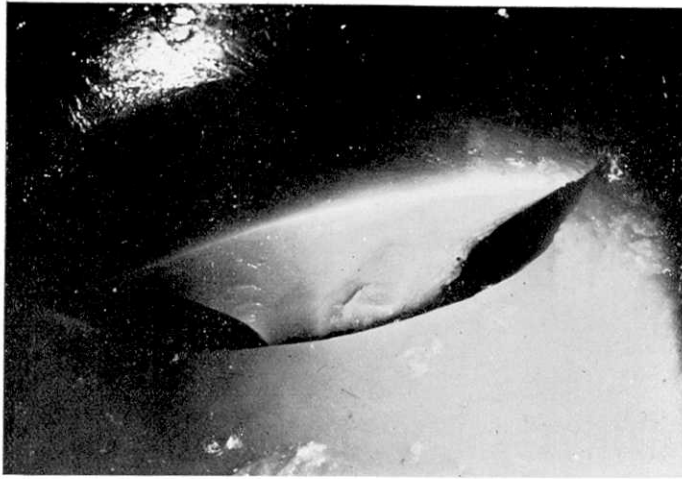


Fig. 11, a.

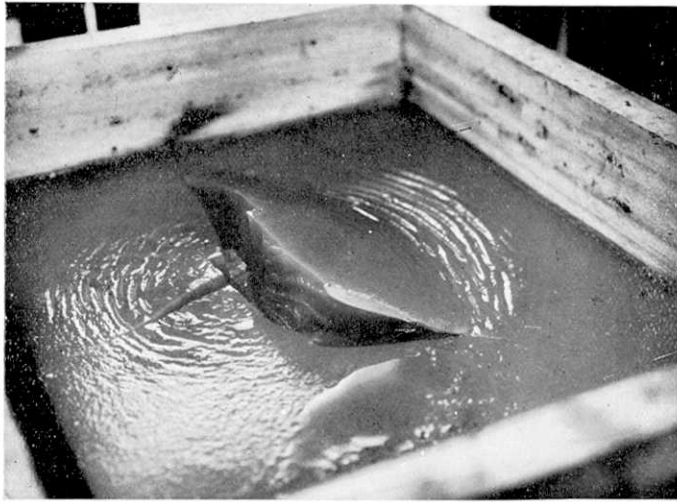


Fig. 11, b.

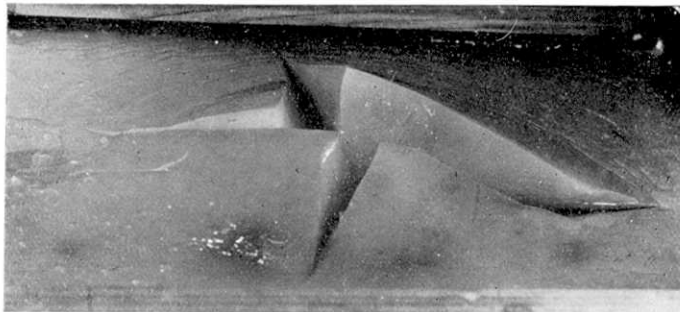


Fig. 11, c.

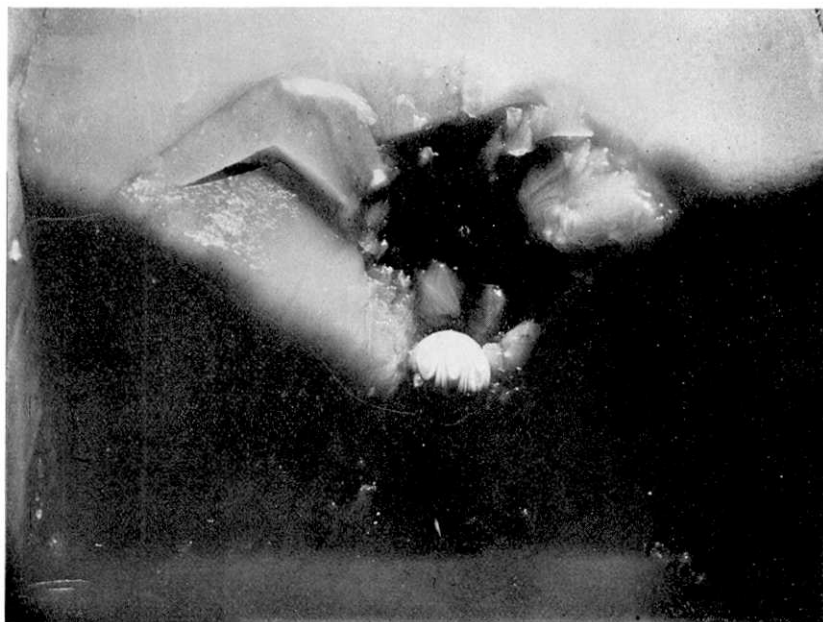


Fig. 11, d.



Fig. 11, e.